

# Microstructural evolution of a PM TiAl alloy during heat treatment in $\alpha+\gamma$ phase field

SU Meike<sup>a</sup>, ZHENG Lijing<sup>a</sup>, LANG Zebao<sup>b</sup>, YAN Jie<sup>a</sup>, and ZHANG Hu<sup>a</sup><sup>a</sup> School of Materials Science and Engineering, Beijing University of Aeronautics and Astronautics, Beijing 100191, China;<sup>b</sup> Aerospace Research Institute of Materials & Processing Technology, Beijing 100076, China

Received 24 February 2012; received in revised form 20 April 2012; accepted 27 May 2012

© The Nonferrous Metals Society of China and Springer-Verlag Berlin Heidelberg 2012

## Abstract

In this study, the effect of temperatures and cooling rates of heat treatment on the microstructure of a powder metallurgy (PM) Ti-46Al-2Cr-2Nb-(B,W) (at.%) alloy was studied. Depending on the cooling rate and temperature, the different structures were obtained from the initial near- $\gamma$  (NG) microstructures by heat treatment in the  $\alpha+\gamma$  field. The results show that the microstructures of samples after furnace cooling (FC) consist primarily of equiaxed  $\gamma$  and  $\alpha_2$  grains, with a few grains containing lamellae. Duplex microstructures consist mainly of  $\gamma$  grains and lamellar colonies were obtained in the quenching into another furnace at 900°C (QFC) samples. However, further increasing of the cooling rate to air cooling (AC) induces the transformation of  $\alpha\rightarrow\alpha_2$  and results in a microstructure with equiaxed  $\gamma$  and  $\alpha_2$  grains, and no lamellar colonies are found.

**Keywords:**  $\gamma$ -TiAl-based alloys; powder metallurgy; heat treatment; duplex structure; phase volume fractions

## 1 Introduction

The two-phase  $\gamma$ -TiAl-based alloys are being considered as potential future materials to replace traditional nickel-based superalloys for some high-temperature aeroengine applications [1–2]. It has gained by far its largest interest, owing to its high specific strength at certain elevated temperature, low density, high modulus, and high resistance to creep and oxidation [3–6]. However, the low ductility at room temperature of TiAl alloys is still a problem that needs to be resolved to enable successful application of these alloys in the aeronautical industry [7–8]. In general, TiAl alloys are fabricated by casting and ingot metallurgy (IM) [9]. However, these processes may bring coarse-grained lamellae, a sharp casting texture, and chemical inhomogeneity to the microstructure [10]. Compared with common IM, powder metallurgy (PM) technique has advantage in eliminating composition segregation, realizing the macro net-shape forming, and can effectively solve the difficulty in TiAl alloy shaping [11]. At the present stage, PM technique has attracted more and more interest and numerous works have been conducted on TiAl alloys. However, there is little information about microstructure control works by heat treatment that was reported on PM processing when compared to

IM-processed alloys. Duplex and fully lamellar microstructures are two typical microstructures of  $\gamma$ -TiAl-based alloys and have received the most attention. In general, fine and homogeneous duplex structures result in good ductility and some studies have been carried out on the duplex TiAl alloys [12–13]. The aim of the present work is to study the microstructural evolution of a PM Ti-46Al-2Cr-2Nb-(B,W) (at.%) alloy during heat treatment in the  $\alpha+\gamma$  phase field. The effects of the cooling rate and temperature on the microstructure were investigated.

## 2 Experimental

The alloy used in this study had a nominal composition of Ti-46Al-2Cr-2Nb-(B,W) (at.%). Prealloyed Ti-46Al-2Cr-2Nb powder with a small B,W addition was HIPed at temperatures of 1200 °C at a pressure of 150 MPa for 4 h. The specimens with  $\Phi 12$  mm $\times$ 10 mm were prepared by electric discharge machining from the initial PM ingot and were heat treated in a box furnace. Heat treatment routes are shown as follows:

HT 1: The samples were heated to 1260, 1280, and 1300 °C for 2 h and then furnace cooled (FC) to 900 °C followed by air cooling (AC).

HT 2: The samples were heated to 1260, 1280, and 1300 °C for 2 h and then quenched into another furnace at 900 °C (QFC) followed by AC.

HT 3: The samples were heated to 1260, 1280, and 1300 °C for 2 h then air cooled.

These types of heat treatment are schematically depicted in Fig. 1 and described in Table 1.

Metallographic specimens prepared by standard mechanical polishing method were etched in a mixed solution of 90 ml H<sub>2</sub>O, 30 ml HNO<sub>3</sub>, and 10 ml HF. The microstructures were studied by a CS-3400 scanning electron micro-

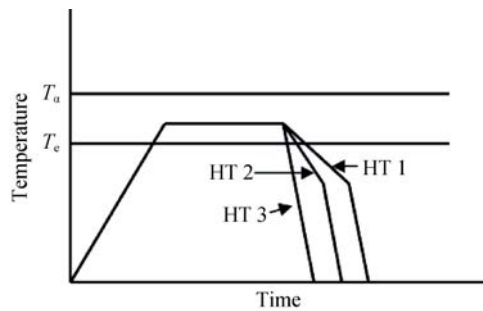


**Fig. 1** Schematic temperature-time path used for different types of heat treatment

**Table 1** Types of heat treatments conducted on specimens (FC: furnace cooling; QFC: quenching into a furnace at 900 °C; AC: air cooling)

Routes	Samples	Heat treatment
HT 1	1	1260 °C/2 h+FC to 900°C+AC
	2	1280 °C/2 h+FC to 900°C+AC
	3	1300 °C/2 h+FC to 900°C+AC
HT 2	1	1260 °C/2 h+QFC+AC
	2	1280 °C/2 h+QFC+AC
	3	1300 °C/2 h+QFC+AC
HT 3	1	1260 °C/2 h+AC
	2	1280 °C/2 h+AC
	3	1300 °C/2 h+AC

scope. A linear intercept method was used to obtain the statistics on the phase volume fractions.

### 3 Results and discussion

The initial PM Ti-46Al-2Cr-2Nb-(B,W) alloy has a near- $\gamma$  (NG) microstructure with  $\sim 10 \mu\text{m}$  grain size. It contains small amounts of  $\alpha_2$  phases appearing white in back-scatter electron imaging (Fig. 2).

In the case of HT 1 involving FC, Fig. 3 shows microstructures of the samples that are furnace cooled from different temperatures. After heating at 1260 °C, the microstructure is still NG microstructure similar to the initial microstructure. However, it contains more  $\alpha_2$  phase, as shown in Fig. 3(a), with white contrast. Increasing heat treatment temperature to 1280 °C results in a microstructure with  $\gamma$  and  $\alpha_2$  grains as the majority phases, and small lamellar colonies are also present (Fig. 3(b)). A similar microstructure dominated by  $\gamma$  and  $\alpha_2$  grains is obtained for the sample heat treated at 1300 °C, as shown in Fig. 3(c).

In the case of HT 2 involving QFC, the microstructures obtained for three heat treatment temperatures are the duplex microstructure, with  $\gamma$  grains and lamellar colonies as the

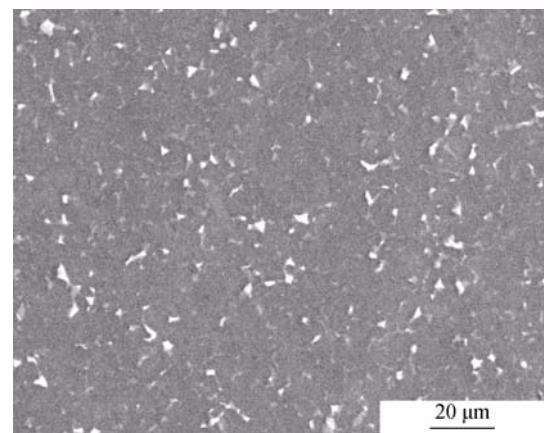


**Fig. 2** BSE image of PM Ti-46Al-2Cr-2Nb-(B,W) alloy

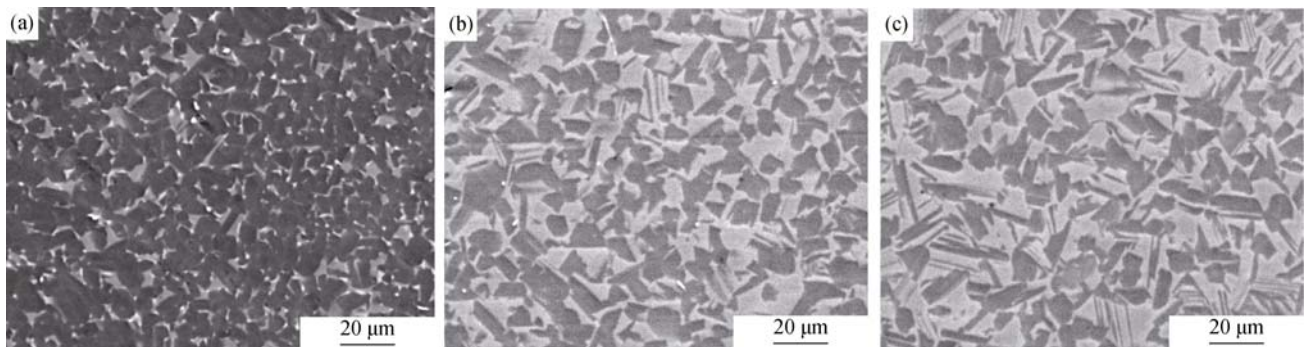


**Fig. 3** BSE images of alloy with HT 1 (a) 1260 °C; (b) 1280 °C; (c) 1300 °C

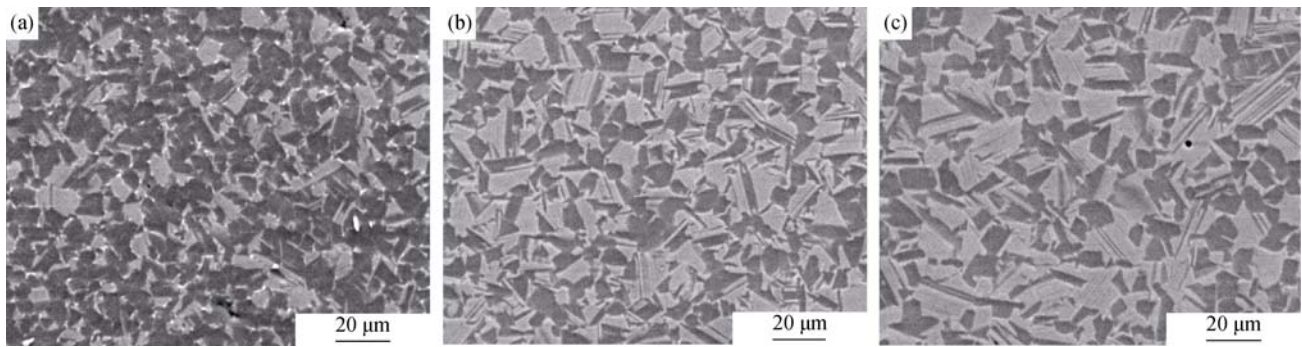


**Fig. 4** BSE images of alloy with HT 2 (a) 1260 °C; (b) 1280 °C; (c) 1300 °C

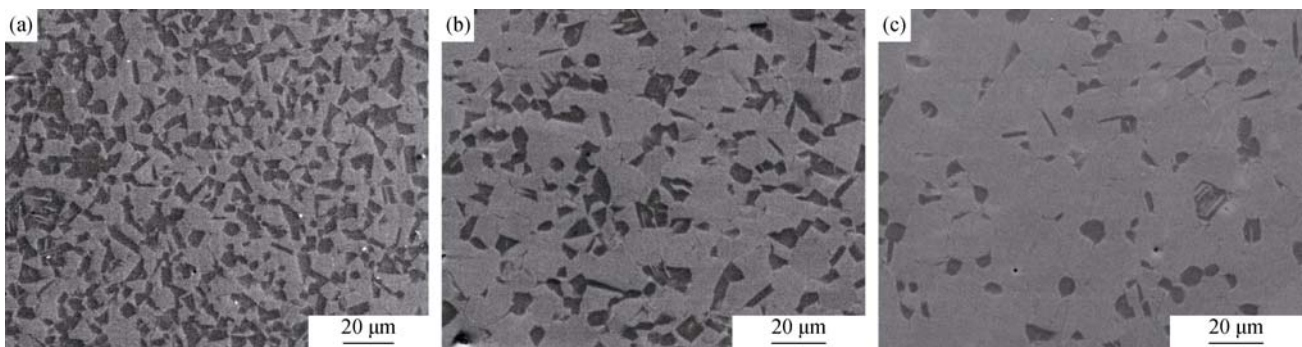


**Fig. 5** BSE images of alloy with HT 3 (a) 1260 °C; (b) 1280 °C; (c) 1300 °C

majority phases, and small amounts of  $\alpha_2$  grains are also present (Fig. 4). It is shown that the volume of lamellar structure increases with increasing heat treatment temperature. As increasing heat treatment temperatures, the grains turn to be slightly coarser.

The highest cooling rate of AC (HT 3) leads to microstructures with  $\gamma$  and  $\alpha_2$  grains, and no lamellar colonies were found. Figure 5 shows the images of heat-treated alloys by AC. The light contrast depicts the  $\alpha_2$  phase and the dark contrast represents the  $\gamma$  phase. Equiaxed  $\gamma$  grains are retained and a greater number of  $\alpha_2$  grains are formed after heat treatment. No lamellar colonies in the treated samples indicate that no lamellar structure is formed during AC after heat treatment.

Figure 6 shows the variation of phase volume fractions after heat treatment at different temperatures followed by HT 1. The FC results in an increase in  $\alpha_2$  and lamellar grain fractions with increasing temperature; for heat treatment temperatures of 1260, 1280, and 1300 °C,  $\alpha_2$  fractions are 12.0%, 49.0%, and 49.9% and lamellar-colony fractions are 0.0%, 9.0%, and 12.9%, respectively.  $\gamma$  fractions decrease with increasing temperature, whereas  $\gamma$  fractions are 88.0%, 42.0%, and 37.2%, respectively.

In the case of the HT 2 involving QFC, it can be seen in Fig. 7 that the increase of temperature makes the  $\gamma$  and  $\alpha_2$

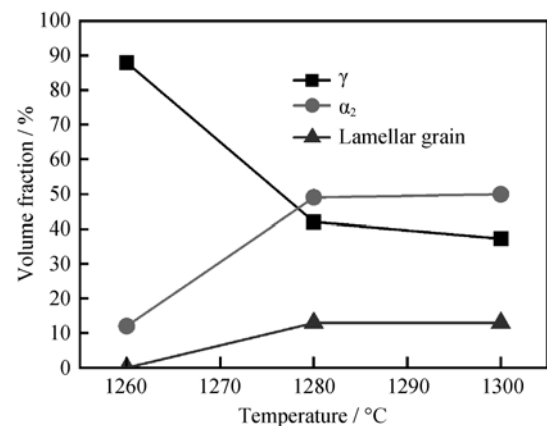


**Fig. 6** Variation of phase volume fractions with temperature after heat treatment of HT 1

fractions decrease. For heat treatment temperatures of 1260, 1280, 1300 °C,  $\gamma$  fractions are 69.0%, 38.6%, and 35.0% and  $\alpha_2$  fractions are 49.9%, 9.0%, and 5.9%, respectively. Lamellar-colony fractions increase with increasing temperature, which are 22.0%, 55.5%, and 60.0%, respectively.

Figure 8 shows the variation of phase volume fractions with temperature obtained at cooling rate of AC (HT 3). It can be seen that the increase of temperature makes  $\gamma$  fractions decrease.  $\alpha_2$  fractions increase with increasing temperature for heat treatment temperatures of 1260, 1280, and

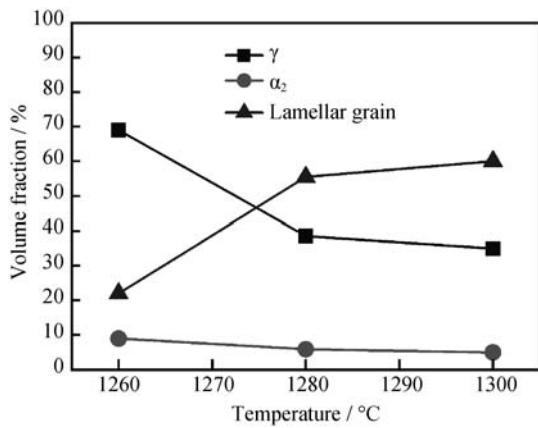


Fig. 7 Variation of phase volume fractions with temperature after heat treatment of HT 2

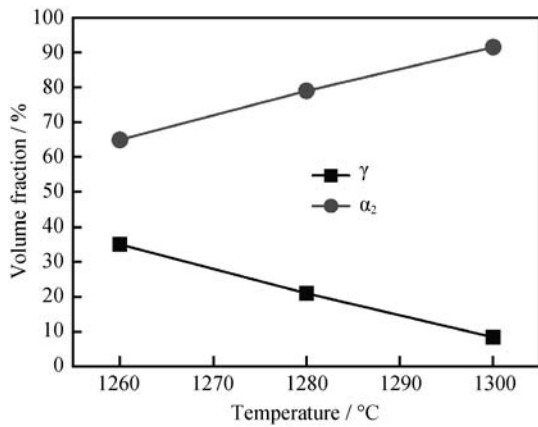


Fig. 8 Variation of phase volume fractions with temperature after heat treatment of HT 3

1300 °C.  $\gamma$  fractions are 35.1%, 21.0%, and 8.4%, whereas  $\alpha_2$  fractions are 64.9%, 79.0%, and 91.6%, respectively.

In addition to temperature, the cooling rate is also an important factor affecting the morphology of transformation products. Figures 9 to 11 show the phase composition with different cooling rates at 1260, 1280, and 1300 °C, respectively. After heat treatment at 1260 °C, the microstructures contain  $\gamma$  and  $\alpha_2$  grains for the alloys cooled by FC and AC, and one of the two phases turns to be the dominant microstructure. The cooling rate of QFC results in a three-phase microstructure, with  $\gamma$  as the majority phase and lamellar colonies and  $\alpha_2$  grain (Fig. 9).

The phase composition of the samples heat treated at 1280 and 1300 is similar. AC leads to a microstructure containing  $\gamma$  and  $\alpha_2$  grains and a higher fraction of  $\alpha_2$  grains (Figs. 10 and 11). After FC and QFC, three-phase microstructures are obtained consisting of equiaxed  $\gamma$  grains, lamellar colonies, and  $\alpha_2$  grains. The microstructure of QFC samples exhibit higher amounts of lamellar colonies than the samples cooled by FC; consequently, the amounts of  $\alpha_2$  grains decrease.

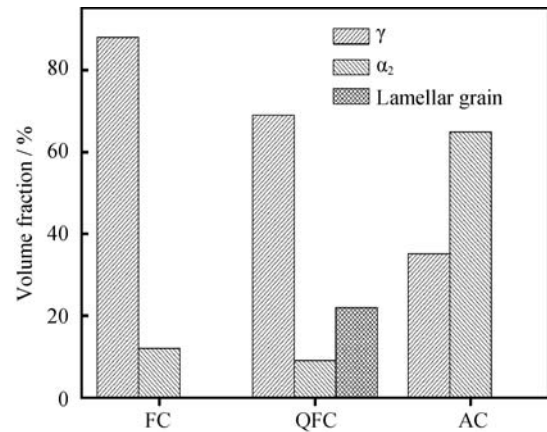


Fig. 9 Phase volume fractions of microstructures after heat treatment at 1260 °C with different cooling rates

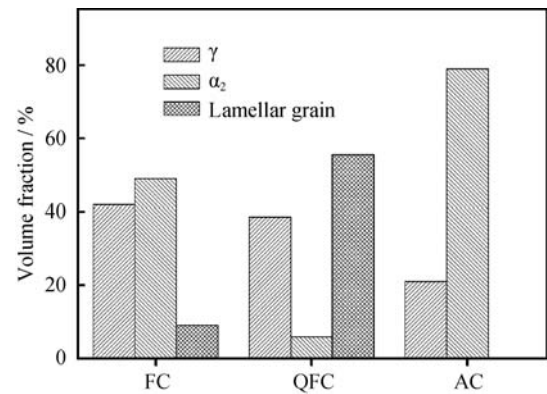


Fig. 10 Phase volume fractions of microstructures after heat treatment at 1280 °C with different cooling rates

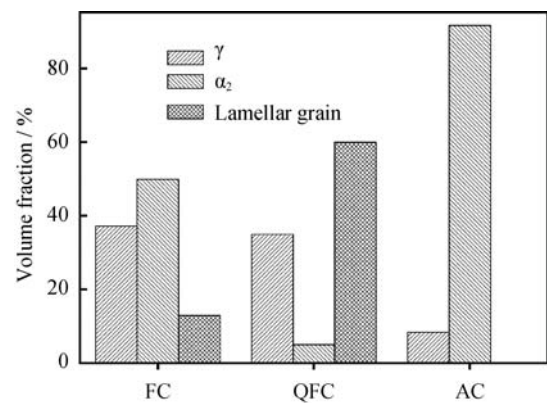


Fig. 11 Phase volume fractions of microstructures after heat treatment at 1300 °C with different cooling rates

It is well known that the duplex structure in as-cast samples is always formed through thermomechanical processing. In this case, the recrystallisation and conversion of the lamellar microstructure to duplex structure require significant amounts of energy. These morphological developments cannot be induced in a reasonable amount of time by simply heat treating, and the additional strain energy imparted by

thermomechanical processing (e.g., extrusion or forging) is often required [14].

In the present study, the initial NG structure is heated to a temperature in  $\alpha+\gamma$  phase field. During these treatments, the two mechanisms of the transformation can occur. (1)  $\gamma\rightarrow\alpha$  reaction resulted in the formation of  $\alpha$  phase with different crystallographic orientations in the  $\gamma$  matrix because  $\alpha$  plate could precipitate from  $\gamma$  in parallel to either of the four  $\{111\}$  planes. (2)  $\alpha_2$  particles, formed at  $\gamma$  grain boundaries in the course of prior powder consolidation, grow into  $\alpha$  grain during heat treatment [15]. According to the lever rule, the amount of  $\alpha$  phase varies with the change of aging temperature in the ( $\alpha+\gamma$ ) phase region, and  $\alpha$  phase develops; thus, an equilibrium  $\alpha$  volume fraction is achieved [16]. In the subsequent cooling process, it has been shown in this study that the highest cooling rate such as AC resulted in the transformation of  $\alpha\rightarrow\alpha_2$  regardless if the temperature is 1260, 1280, or 1300 °C. The transformation of  $\alpha\rightarrow\alpha_2$  always takes place in IM when the cooling rate is so high such as oil quench (OQ) [17]. The detailed observations reveal that the microstructure after AC is  $\gamma+\alpha_2$  dual-phase structure and that no  $\gamma$  plates could be observed in  $\alpha_2$  grains (Fig. 5). In FC and QFC samples, it is can be seen that lamellar structure appears in the structures. Kim [18] reported that lamellae were formed in a forged IM  $\gamma$ -TiAl alloy via  $\alpha$  plates growing into  $\gamma$  matrix during heat treatment at temperatures in the  $\alpha+\gamma$  phase field (type III lamellae), and these lamellar structures were formed from  $\alpha$  phase during cooling after heat treatment at temperatures near or above  $T_a$  (type I lamellae). In the present investigation, the lamellar structure in the duplex structures could be formed via type I reactions. It is shown that the structure without lamellar structure before cooling (Fig. 5). This indicates that lamellar structure is formed during cooling via the precipitation of  $\gamma$  plates in the prior  $\alpha$  grains when cooling by cooling rate of QFC or FC (Figs. 3 and 4).

It has been shown in this study that cooling rate and temperature affect the microstructure. With the increase of temperature and cooling rate, the volume fraction of lamellar colonies increases. For FC case, it seems that the microstructure of samples after heat treatment consists primarily of equiaxed  $\gamma$  and  $\alpha_2$  grains with a few grains containing lamellae (Fig. 3). The microstructures are the dual-phase microstructure but with the additional presence of a few lamellar colonies. When the cooling rate is increased to QFC, duplex microstructures consists primarily of equiaxed  $\gamma$  grains and lamellar colonies are formed during cooling via the precipitation of  $\gamma$  plates in the prior  $\alpha$  grain. It has been well established that the lamellar structure formed by precipitation of  $\gamma$  laths in  $\alpha$  matrix by “terrace-ledge-kink” mechanism [19] and it has everything to do with atom diffusion [20]. A

longitudinal and lateral growth of the lamellar precipitates occurs through the “terrace-ledge-kink” mechanism, which corresponds to the transfer of atoms onto ledge-kinks, ensuring that the composition change is involved in the lamellar structure formation [21]. When the cooling rate and temperature are higher, the driving force for formation of lamellar structure increases and more atoms transfer to ensure the change of components for lamellar structure formation, which is of great benefit to the occurrence of transformation  $\alpha\rightarrow\alpha_2+\gamma$  and more lamellar colonies can be obtained. With decreasing cooling rate and temperature, the occurrence of lamellar structure transformation becomes difficult because the formation of the lamellar  $\gamma$  phase slows down and can stop by reducing the driving force for the ledge movement. However, further increasing cooling rate to AC will result in a transformation of  $\alpha\rightarrow\alpha_2$  because the cooling rate is too high and there is no time for formation of lamellar structure.

The absence of lamellar structure is due to the high cooling rate in AC case. It should be noted that the small grain size of the dual-phase structure is also responsible for the absence of lamellar structure. Although the underlying reason is not well understood and should be studied further, it can be seen that lamellar structure always exists in grains with a grain size of  $>10\ \mu\text{m}$  and  $\alpha_2$  grain size of  $<5\ \mu\text{m}$  in all cases of FC and QFC.

#### 4 Conclusion

This study reports the effect of temperature and cooling rate on the microstructure of a PM Ti-46Al-2Cr-2Nb-(B,W) (at.%) alloy by heat treatment. The lamellar structure can form via the precipitation of  $\gamma$  plates in the prior  $\alpha$  grains in FC and QFC samples, whereas AC leads to all  $\alpha$  grains simply ordered to  $\alpha_2$  grain and no  $\gamma$  plates could be observed in  $\alpha_2$  grains.

In the case of HT 1 involving FC, the microstructures of samples after heat treatment consist primarily of equiaxed  $\gamma$  and  $\alpha_2$  grains, with a few grains containing lamellae. With increasing temperature, the volume fractions of lamellar colonies and  $\alpha_2$  grains increase and  $\gamma$  fractions decrease. For heat treatment temperatures of 1260, 1280, and 1300 °C,  $\alpha_2$  fractions are 12.0%, 49.0%, and 49.9%, lamellar-colony fractions are 0.0%, 9.0%, and 12.9%, and  $\gamma$  fractions are 88.0%, 42.0%, and 37.2%, respectively.

In the case of HT 2 involving QFC, the duplex microstructures obtained consist mainly of  $\gamma$  grains and lamellar colonies, and small amounts of  $\alpha_2$  grains are also present. With increasing temperature, the volume fractions of  $\gamma$  and  $\alpha_2$  grains decrease and lamellar-colony fractions increase. For heat treatment temperatures of 1260, 1280, and 1300 °C,

$\gamma$  fractions are 69.0%, 38.6%, and 35.0%,  $\alpha_2$  fractions are 49.9%, 9.0%, and 5.9%, and lamellar-colony fractions are 22.0%, 55.5%, and 60.0%, respectively.

In the case of HT 3, the microstructures after AC are  $\gamma+\alpha_2$  structures with no lamellar colonies. With increasing temperature,  $\alpha_2$  grain fractions increase and  $\gamma$  grain fractions decrease. For heat treatment temperatures of 1260, 1280, and 1300 °C,  $\gamma$  fractions are 35.1%, 21.0%, and 8.4% and  $\alpha_2$  fractions are 64.9%, 79.0%, and 91.6%, respectively.

## Acknowledgement

This project was financially supported by the National Natural Science Foundation of China (No. 51101003).

## References

- [1] Kim Y.W., Progress in the understanding of gamma titanium aluminides, *JOM*, 1991, **43** (8): 40.
- [2] Takeyama M., Microstructural evolution and tensile properties of titanium-rich TiAl alloy, *Mater. Sci. Eng. A*, 1992, **152** (1-2): 269.
- [3] Su Y.Q., Liu X.W., Luo L.S., Zhao L., Guo J.J., and Fu H.Z., Deoxidation of Ti-Al intermetallics via hydrogen treatment, *Int. J. Hydrog. Energy*, 2010, **35** (17): 9214.
- [4] Su Y.Q., Liu C., Li X.Z., Guo J.J., Li B.S., Jia J., and Fu H.Z., Microstructure selection during the directionally peritectic solidification of Ti-Al binary system, *Intermetallics*, 2005, **13** (3-4): 267.
- [5] Su Y.Q., Guo J.J., Jia J., Liu G.Z., and Liu Y., Composition control of a TiAl melt during the induction skull melting (ISM) process, *J. Alloy. Compd.*, 2002, **334** (1-2): 261.
- [6] Kim Y.W., Ordered intermetallic alloys, part III: gamma titanium aluminides, *JOM*, 1994, **46** (7): 30.
- [7] Lu X., Zhu L.P., Liu C.C., Zhang L., Wu M., and QU X.H., Fabrication of micro-fine high Nb-containing TiAl alloyed powders by fluidized bed jet milling, *Rare Metals*, 2012, **31** (1): 1.
- [8] Kim Y.W., Intermetallic alloys based on gamma titanium aluminide, *JOM*, 1989, **41** (7): 24.
- [9] Toshimitsu T., Manufacturing technology for gamma-TiAl alloy in current and future applications, *Rare Metals*, 2011, **30** (S1): 294.
- [10] Imayev R.M., Imayev V.M., Oehring M., and Appel F., Alloy design concepts for refined gamma titanium aluminide based alloys, *Intermetallics*, 2007, **15** (4): 451.
- [11] Yang S.H., Kim W.Y., and Kim M.S., Fabrication of unidirectional porous TiAl-Mn intermetallic compounds by reactive sintering using extruded powder mixtures, *Intermetallics*, 2003, **11** (8): 849.
- [12] Chu W.Y., and Thompson A.W., Effect of grain size on yield strength in TiAl, *Scripta Metall.*, 1991, **25** (3): 641.
- [13] Koeppel C., Bartels C., Seege J., and Mecking H., General aspects of the thermomechanical treatment of two-phase intermetallic TiAl compounds, *Metall. Mater. Trans. A*, 1993, **24A** (8): 1795.
- [14] Arno B., Carsten K., and Heinrich M. Microstructure and properties of Ti-48Al-2Cr after thermomechanical treatment. *Materials Science and Engineering A*, 1995, **192-193** (1): 226.
- [15] Zhang G., Blenkinsop P.A., and Wise M.L.H., Phase transformations in HIPed Ti-48Al-2Mn-2Nb powder during heat-treatments, *Intermetallics*, 1996, **4** (6): 447.
- [16] Flower H.M., and Christodoulou J., Phase equilibria and transformations in titanium aluminides, *Mater. Sci. Technol.*, 1999, **15** (1): 45.
- [17] Denquin A., and Naka S., Phase transformation mechanism involved in two phase TiAl-II: discontinuous coarsening and massive-type transformation, *Acta Metall.*, 1996, **44** (1): 353.
- [18] Kim Y.W., Microstructural evolution and mechanical properties of a forged gamma titanium aluminide alloy, *Acta Metall. Mater.*, 1992, **40** (6): 1121.
- [19] Aaronson H.I., Atomic mechanisms of diffusional nucleation and growth and comparisons with their counterparts in shear transformations, *Metall. Mater. Trans. A*, 1993, **24** (2): 241.
- [20] Mishin Y., and Herzig C., Dislocation in the Ti-Al system, *Acta Metall.*, 2000, **48** (2): 589.
- [21] Denquin A., and Naka S., Phase transformation mechanism involved in two phase TiAl-I: lamellar structure formation, *Acta Metall.*, 1996, **44** (1): 343.